PAPER

Platinum (II) complexes and their nanoformulations: preparation, characterisation and cytotoxicity

Platinum (II) complexes and their nanoformulations: preparation, characterisation and cytotoxicity

Thi Hong Tuyet Phan[1], Thi Thu Huong Le[2,3], Ke Son Phan[2], Thi Lan Anh Tran[2], Hoa Du Nguyen[1], The Tam Le[1], Thi Tuong Vi Bui[1], Mai Huong Le[4], Thi Hong Ha Tran[4], Duc Huy Luu[5] and Phuong Thu Ha[2]

[1] Vinh University, 182 Le Duan, Vinh City, Nghe An, Vietnam

[2] Institute of Materials Science, Vietnam Academy of Science and Technology, 18 Hoang Quoc Viet, Cau Giay, Hanoi, Vietnam

[3] Vietnam National University of Agriculture, Trau Quy, Gia Lam, Hanoi, Vietnam

[4] Institute of Natural Products Chemistry, Vietnam Academy of Science and Technology, 18 Hoang Quoc Viet, Cau Giay, Hanoi, Vietnam

[5] Institute of Chemistry, Vietnam Academy of Science and Technology, 18 Hoang Quoc Viet, Cau Giay, Hanoi, Vietnam

E-mail: tuyetph@vinhuni.edu.vn, lethithuhuong@vnua.edu.vn and thuhp@ims.vast.ac.vn

Abstract

Development of novel drugs or drug delivery systems has attracted much attention of researchers. In this study, we aimed to prepare 2 new Pt(II) complexes with thiosemicarbazone and their nanoformulations for cancer treatment application. Pt(II)-camphor thiosemicarbazone/ P1 and Pt(II)-camphor 4-phenyl thiosemicarbazone/P2) were successfully prepared and structurally confirmed by MS, IR, 1H-NMR, UV–vis spectroscopies and thermal analysis. From the complexes, 2 PLGA-based nanoformulations (nP1 and nP2) were synthesised with the average size of 50 nm by emulsification/evaporation method and investigated for their toxicity against Hep-G2, LU-1 and RD cancer cell lines. The results show that the Pt(II) complexes and their nanoformulations were potential for chemotherapy.

Supplementary material for this article is available online

1. Introduction

Platinum (II) complexes are widely used as anticancer agents, both in biomedical investigations and in clinic for treatment of many cancer types [1]. However, the systemic toxicities such as nausea, ototoxicity, renal impairment and neurotoxicity restrict their treatment efficacy [2–4]. Therefore, it is essential to find out new Pt(II) complexes and effectively use the complexes in cancer treatment. Using a number of natural bioactive molecules as ligands in Pt(II) complexes has attracted much attention of researchers in recent years [5–7]. Novel approach of encapsulating Pt(II) complexes onto nanocarriers in order to increase the drug selectivity and reduce the systemic side effects has also been investigated [8–10]. The nanocarriers can be prepared in different manners by loading the cancer drugs into liposomes, lipid emulsions or polymeric micelles [8, 11, 12]. Among these, polymers provide the Pt(II) complexes with the steric effect that helps to prolong the retention time of the polymeric nanocarriers, reduce toxicology but maintain the antitumor activity both *in vivo* and *in vitro* [13, 14].

In our previous works, we synthesised camphor methyl [15] or menthone [16] thiosemicarbazone Pt(II) complexes. In this study, we aimed to synthesise 2 new Pt(II) complexes with camphor thiosemicarbazone and camphor 4-phenyl thiosemicarbazone and loaded the complexes into

nanocarriers for cancer treatment application. Camphor is an Asian traditional medicine with high bioactivity of anti-inflammation, antibacteria, etc [17]. Its thiosemicarbazone derivatives possess interesting reactions [18, 19]. Most complexes of thiosemicarbazone have biological activity but the relationship between structure and activity is unclear [20]. Recently, camphor thiosemicarbazone has been used to coordinate with Cu(II), Zn(II) and Pd(II). The complexes had IC$_{50}$ values in the range of 9.8 to 14.0 μM on MCF-7 cells [21]. However, the coordination of camphor and its thiosemicarbazone derivatives with platinum could create new complexes. In terms of using nanocarriers, nanomaterials from camphor have also been reported [22]. In this report, PLGA (Poly (lactic-co-glycolic acid)), one of the most widely used biodegradable copolymer that is suitable for nano-drug delivery systems [23], was used for loading the synthesised complexes. Our results has contributed to clarifying the structure-activity relationship of camphor thiosemicarbazone Pt(II) complexes and their nanoformulations.

2. Materials and methods

2.1. Materials

Camphor, thiosemicarbazide, 4-phenyl thiosemicarbazide, acetic acid, ethanol, PLGA and PVP (Polyvinylpyrrolidone) were purchased from Merck, K$_2$[PtCl$_4$] was purchased from Sigma-Aldrich.

2.2. Method

2.2.1. Synthesis of thiosemicarbazone derivatives. The synthesis of thiosemicarbazone derivatives and their Pt(II) complexes was similar to a published procedure for camphor methyl thiosemicarbazone synthesis [15] and listed below.

2.2.2. Synthesis of camphor thiosemicarbazone (Hthiocam). Hthiocam was synthesised from 0.01 mol thiosemicarbazide (0.91 g) and 0.01 mol camphor (1.52 g). The reactants were dissolved in warm ethanol. pH of the solution was adjusted to 3–4 by adding anhydrous acetic acid. The reaction was allowed to occur under continuous stirring and reflux at 70 °C for 6 h. The obtained crystals were then separated, washed and dried in a desiccator. The final product, denoted as Hthiocam, was a white powder (1.96 g, reaction yield: 87%).

   (a) Synthesis of camphor 4-phenyl thiosemicarbazone (H4thiocam)

   H4thiocam was synthesised in the same procedure with the synthesis of Hthiocam except for the replacement of 0.01 mol thiosemicarbazide by 0.01 mol

4-phenyl thiosemicarbazide (1.67 g) and the reaction time was prolonged to 8 h. H4thiocam synthesis had the yield of 83% (2.49 g H4thiocam obtained).

   (b) Synthesis of Pt (II) complexes

Pt(II) complexes were obtained from the reaction of the thiosemicarbazone derivatives with K$_2$[PtCl$_4$] solution. In brief, 50 ml water solution of 0.02 M K$_2$[PtCl$_4$] solution was reacted with 100 ml ethanol solution of 0.02 M Hthiocam or H4thiocam at the temperature of 40 °C with magnetic stirring for 1 h. The solutions were then kept at room temperature of 25 °C for 24 h to precipitate the complexes. The precipitates were isolated and washed with water and ethanol before drying in a dessicator. The obtained Pt(II) complexes were yellow powders and denoted as Pt-thiocam (P1) or Pt-4thiocam (P2). The reaction yields were 89% and 92% for P1 and P2, respectively.

2.2.3. Synthesis of PLGA Pt complex loaded nanoparticles. PLGA Pt complex loaded nanoparticles were prepared by emulsification/evaporation method. Firstly, 5 mg of Pt-thiocam or Pt-4thiocam and 50 mg PLGA polymer were dissolved in 100 ml acetone. The solution was then added dropwise into aqueous solution of PVP 1% (w/v) under continuous stirring at room temperature for 24 h. Then, the mixture was gently stirred overnight to evaporate the organic solvent completely. Finally, nanoparticle suspensions were obtained after removing the uncapped Pt complexes by centrifugation at 5000 rpm for 5 min and stored at room temperature. The P1 and P2 loaded nanoparticles were denoted as nP1 and nP2, respectively.

2.2.4. Structure determination. The structures of the thiosemicarbazone derivatives and their complexes were determined by mass spectroscopy with electrospray ionisation technique (ESI-MS) in an Agilent 1100 LC/MSD Trap. The IR spectra of the samples were also recorded with a FTIR Shimadzu spectrophotometer using KBr pellet at the frequency range of 4000–400 cm^{-1}. ^{1}H-NMR spectra were recorded by a Bruker 500 MHz spectrometer and the chemical shifts were given in units of δ relative to TMS as an internal standard using DMSO-d6 as the solvent.

Size and morphology of the nanoformulations were measured by field emission scanning electron microscope (FE-SEM) in a Hitachi S-4800. Hydrodynamic size and zeta potential of these samples were obtained by DLS method in a Malvern ZetaSizer. Thermal gravimetric diagrams of the complexes and their nanoformulations were recorded on a TG-DSC Labsys Evo system under inert atmosphere of nitrogen from room temperature to 900 °C.

The encapsulating efficiency (EE%) of Pt complexes onto the nanosuspensions was calculated by the following formulation:

$$EE\,(\%)\;=\;(\text{total weight of Pt complex–weight of uncapped Pt complex})/(\text{total weight of Pt complex}).$$

Adv. Nat. Sci.: Nanosci. Nanotechnol. **12** (2021) 025016

T H T Phan *et al*

Table 1. ESI/MS data and compound's molecular formula.

Sample	m/z, $[M]^+$/$[M + H]^+$	M	Molecular formula
Hthiocam	226	225	$C_{11}H_{19}N_3S$
Pt-thio-cam (P1)	644	643	$Pt(C_{11}H_{18}N_3S)_2$
H4thiocam	302	301	$C_{17}H_{23}N_3S$
Pt-4thio-cam (P2)	795	795	$Pt(C_{17}H_{22}N_3S)_2$

The spectra of Hthiocam, H4thiocam and their complexes showed several informative fragment ions confirming their molecular weights. The molecular ion peaks were confirmed to be $[M]^+$ or $[M + H]^+$.

In which, uncapped Pt complex that was removed from centrifugation was collected, dried and weighed to calculate the EE%.

2.2.5. The cytotoxicity assay. The method of Skehan *et al* [24] and Likhiwitayawuid *et al* [25] was used to determine cytotoxicity of the derivatives, their complexes (P1 and P2) and their nanoformulations (nP1 and nP2) on Hep-G2, LU-1, RD and Vero cell lines. Ellipticine was used as the positive control. The cancer cells were incubated with P1, P2, nP1, nP2 and ellipticine at different concentrations in 96-well plates. After 48 h of treatment, cell survival index was measured and the half maximal inhibitory concentration (IC_{50}) values were calculated for each cell type.

3. Results and discussion

3.1. Thiosemicarbazone derivatives and their complexes

3.1.1. MS analysis. The MS spectra of Hthiocam, H4thiocam and their complexes P1, P2 were shown in figure S1 (available online at stacks.iop.org/ANSN/12/025016/mmedia). The ESI/MS data are presented in table 1.

3.1.2. NMR spectral analysis. In the ^{1}H-NMR spectrum of Hthiocam (figure S2(A)), a singlet at 8.34 ppm was assigned to proton of NH –hydrazine, a doublet at 7.20 ppm and 6.30 ppm was assigned to 2H of NH_2. The signals at 1.20 ppm to 1.40 ppm were assigned to 9 H of CH_3 groups and signals in range 1.19 to 2.63 ppm were assigned to protons of CH and CH_2. A singlet at 10.16 ppm appearing in the ^{1}H-NMR spectrum of H4thiocam (figure S2(C)) can be assigned to the proton in NH-hydrazine group. The proton in the NH-amide exhibits a singlet peak at 9.64 ppm. The signals in range 7.15 to 7.59 ppm were assigned to 5H of phenyl ring. Triplet signals at 0.73 ppm to 1.03 ppm were assigned to 9 H of CH_3 groups and signals in range 1.73 to 2.43 ppm were assigned to protons of CH and CH_2. The appearance of NH signal in spectra of Hthiocam and H4thiocam confirmed that they were in the thione form. In the HNMR spectra of Pt-thiocam (P1) and Pt-4thiocam (P2) (figures S2(B),2(D)), there is no signal corresponding to the proton in NH-hydrazine (in NHC=S group). This is due to the deprotonation of Hthiocam or H4thiocam to bond with Pt(II) via S and N in the complex.
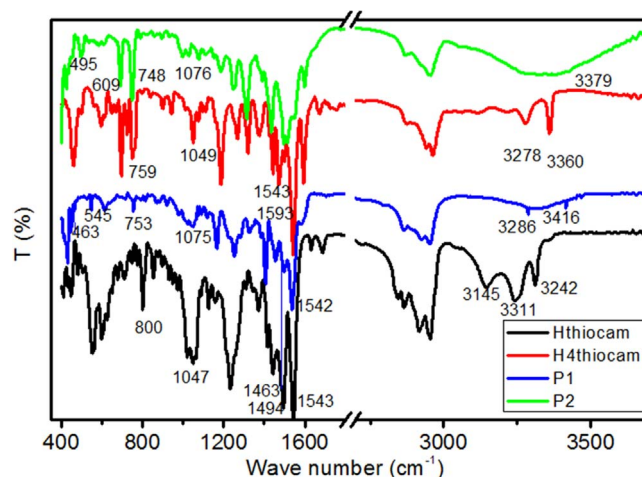
Figure 1. IR spectra of Hthiocam, Pt-thiocam, H4thiocam and Pt-4thiocam.
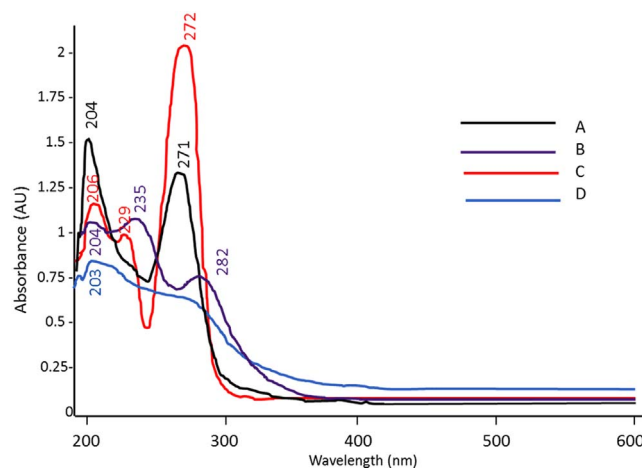
Figure 2. UV–vis spectra of Hthiocam (A) and P1 (B), H4thiocam (C) and P2 (D).

Other signals of P1 and P2 appeared at similar positions compared to those of Hthiocam or H4thiocam. Our results are in good agreement with some previous researches [21, 26].

3.1.3. IR spectra. Typical IR bands of thiosemicarbazone derivatives and their Pt complexes are presented in table 2.

In the IR spectrum of Hthiocam (figure 1), three absorption bands at 3311, 3242 and 3145 cm^{-1} result from the stretching frequencies of NH_2 and NH-hydrazine groups. The absorption band of –C=N group appeared at 1543 cm^{-1}. In the IR spectrum of H4thiocam, absorption bands at 3360 and 3278 cm^{-1} result from the stretching frequencies of NH-amide and NH-hydrazine groups. The absorption band of –C=N group appeared at 1593 cm^{-1}. The absence of the peaks in the 2500–2600 cm^{-1} region (typical for –SH group) and the presence of absorptions at 800 cm^{-1} (in IR spectrum of Hthiocam) and 759 cm^{-1} (in IR spectrum of H4thiocam) (ν(C=S)) reveal that Hthiocam and H4thiocam are in the thione form. Similar, typical peaks appeared in the IR spectrum of their Pt(II) complex. The peaks at 3416, 3286 (in
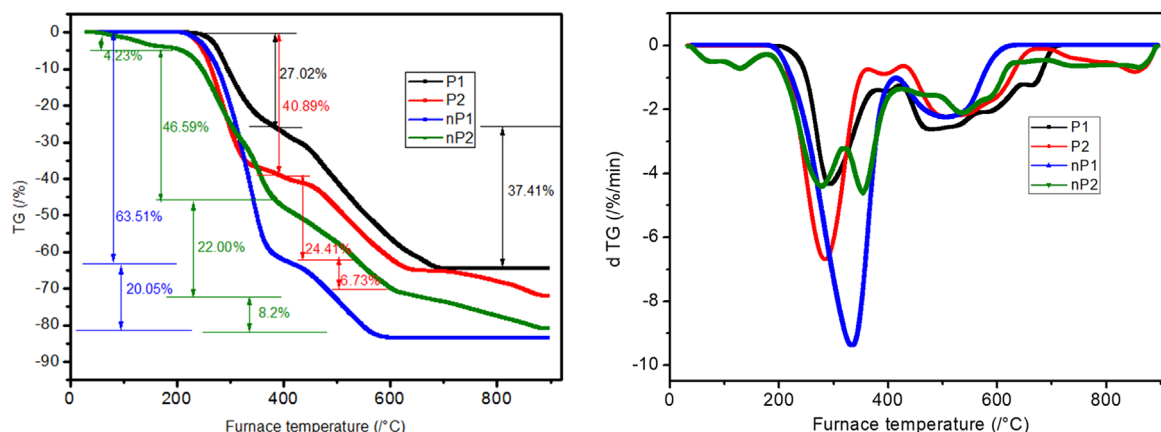
Adv. Nat. Sci.: Nanosci. Nanotechnol. **12** (2021) 025016

T H T Phan *et al*

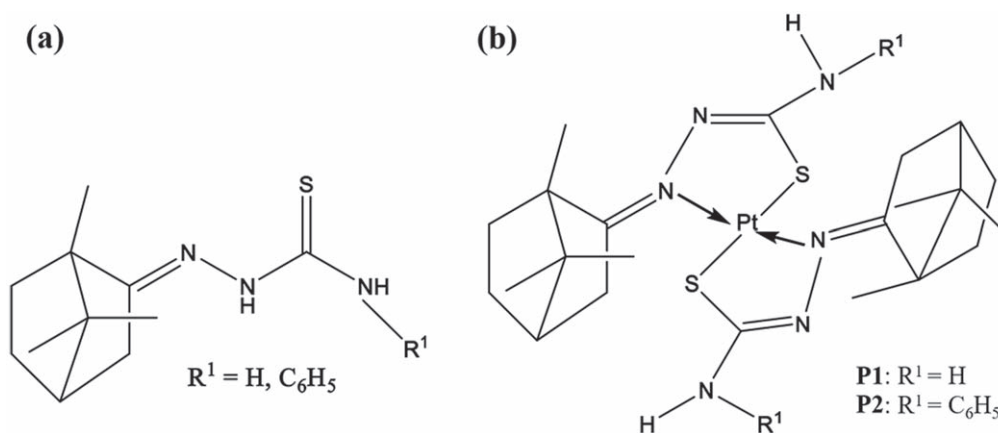**Figure 3.** Thermal analysis results of P1, P2, nP1 and nP2.

Figure 4. Structures of the thiosemicarbazone derivatives (A) and their Pt(II) complexes (B).

Table 2. Selected IR bands (Wavenumber, cm^{-1}) of thiosemicarbazones and Pt(II) complexes.

Compounds	NH	CN + Ar	NN	CS	Pt-X (X = S, N)
Hthiocam	3311, 3242, 3145	1543, 1494	1047	800	—
Pt-thiocam (P1)	3416, 3286	1542, 1463	1075	753	545, 463
H4thiocam	3360, 3278	1593, 1543	1049	759	—
Pt-4thiocam (P2)	3379	1514, 1435	1076	748	609, 495

IR spectrum of P1) and 3379 cm^{-1} (in IR spectrum of P2) are assigned to the NH$_2$ or NH-amide while no absorption band appeared in the 3000–3200 cm^{-1} region (typical for NH-hydrazine). The ν(C=S) band shifted from 800 cm^{-1} or 759 cm^{-1} in the IR spectra of Hthiocam or H4thiocam into 753 cm^{-1} or 748 cm^{-1} in the IR spectrum of their Pt(II)complex. This information suggest that Hthiocam and H4thiocam existing in the thiol form were deprotonated and coordinated to Pt(II) ion through S atom of thiolate group. Another shift from 1593 to 1514 cm^{-1} observed for the C=N group of the free ligand compared to its complex confirmed the coordination of the azomethine nitrogen. In addition, new bands at 545 and 463 cm^{-1} (in IR spectrum of P1) and 609 and 495 cm^{-1} (in IR spectrum of P2) assigned to $\nu_{(Pt-N)}$ and $\nu_{(Pt-S)}$, respectively are evidence for the formation of the Pt(II) complexes.

3.1.4. UV–vis spectra. In the UV–vis spectra (figure 2) of Hthiocam and H4thiocam, there was only absorbance peak within 200 nm to 300 nm range which resulted from the electron transference of π-electron in the ligand molecules. In the spectra of their Pt(II)complexes, these absorbance bands displayed a red shift to the longer wavelength region (200 to 400 nm), showing the change of the ligand from free to complex state. The broad absorbance bands with weak intensity in the 400–450 nm range might be related to the transition of electron from *d* orbital of Pt(II) ion to π* orbital in the ligands [27]. Therefore, the UV–vis results supported the complex formation between Pt(II) ion and Hthiocam or H4thiocam.

The thermal decomposition of P1 occurred in 2 main stages of 200 to 400 °C (with a maximum rate at 293.33 °C)
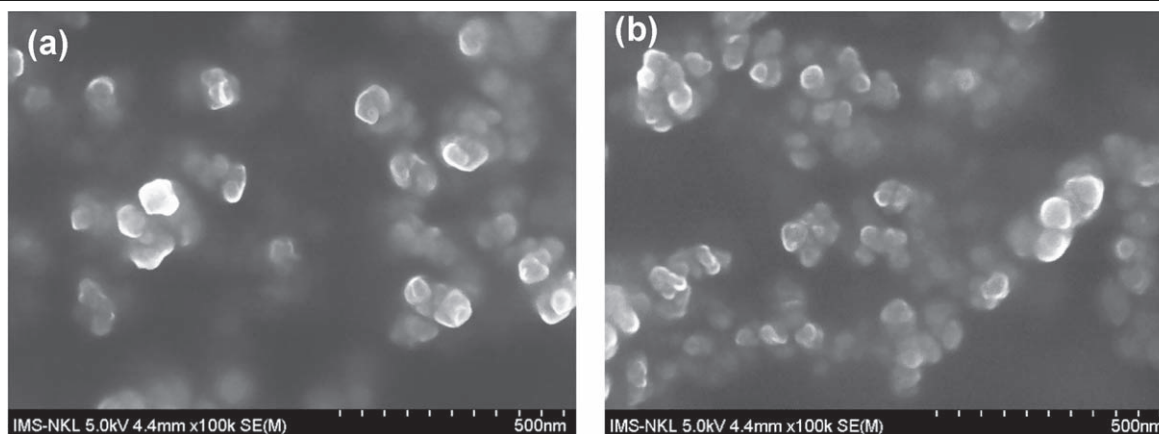
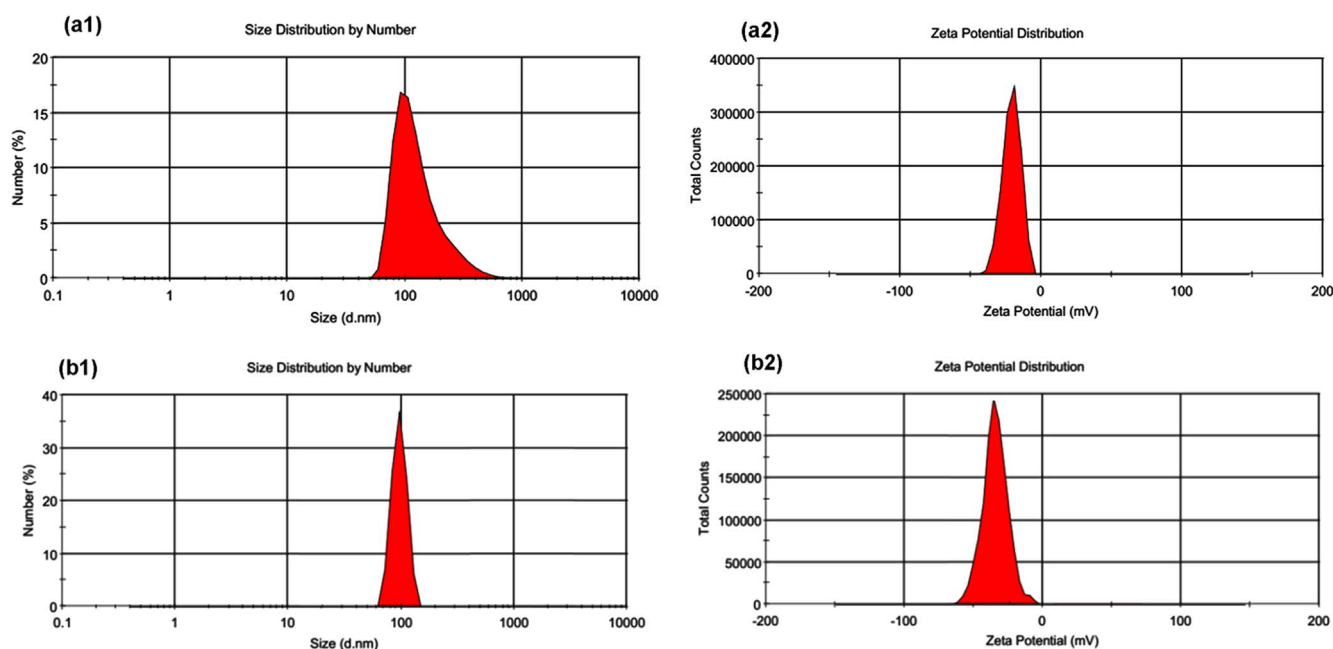**Figure 5.** FE-SEM images of nP1 (A) and nP2 (B).

**Figure 6.** Size distribution and zeta potential of nP1 (A) and nP2 (B).

and 400 to 700 °C with the corresponding weight loss of 27.02 and 37.41%. In addition to 2 similar stages appearing in the P2 decomposition, this complex underwent the third stage of composition at 700 to 900 °C with the weight loss of 6.73% (figure 3). Similar results were observed in other reports on platinum and palladium complexes [28]. The remaining Pt component accounted for 35.57% and 27.97% in P1 and P2, respectively. These results were in good agreement with that calculated from MS spectra (30.28% and 24.53%) and indicated that the complexes were successfully synthesised. Based on the above analysis, reasonable structures of camphor thiosemicarbazone derivatives and their Pt(II) complexes are depicted in figure 4.

3.2. Nanoformulations

FESEM images of nP1 and nP2 nanoformulations are shown in figure 5. As can be seen, PLGA-PVP Pt (II) complex loaded nanoparticles were rather uniform in size (about 50 nm) and had round shape. This small size allows the nanoparticles to prolong the retention time in the body [29]. It also helps the nanoparticles enter the tumour cell through enhanced permeability and retention effect [30]. These properties may contribute to improving the chemotherapeutic properties of nanoformulations in comparison to platinum complex alone.

The thermal analysis diagrams of nP1 and nP2 (figure 3) also confirmed the formation of the nanoformulations with higher content of organic compounds (including the ligands and PLGA, PVP) present in the samples. The encapsulation efficiency (EE%) of P1 and P2 onto the nanoformulations of nP1 and nP2 was calculated to be 78.5 ± 2.3 and 74.1 ± 2.7%, respectively. These numbers confirm that PLGA-PVP were appropriate for Pt(II) complex loading. Some investigators have used PLGA for anticancer hydrophobic drugs including cisplatin and showed similar encapsulating efficiency [23].

Adv. Nat. Sci.: Nanosci. Nanotechnol. **12** (2021) 025016

T H T Phan *et al*
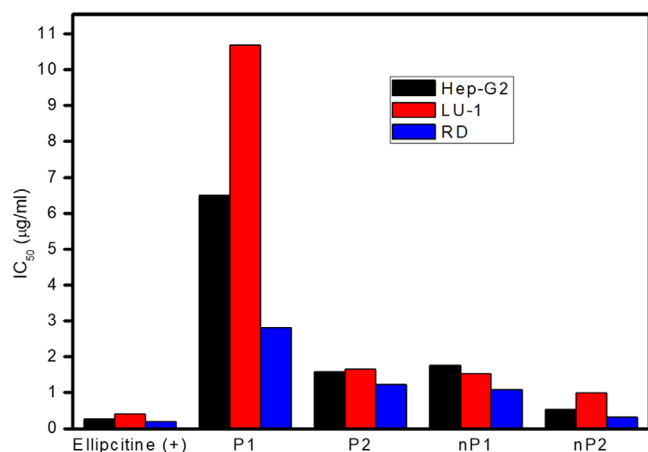
Figure 7. IC_{50} of nanoformulations nP1 and nP2 in comparison with their complexes and positive control of ellipticine.

Table 3. The cytotoxic activity of Pt(II) complexes and their nanoformulations on Hep-G2, LU-1, RD and Vero cells.

No	Sample	IC_{50} (μg ml^{-1})			
		Hep-G2	LU-1	RD	Vero
	Ellipticine (+)	0.27	0.41	0.18	4.09
1	Hthiocam	>50	>50	>50	>50
2	H4thiocam	>50	>50	>50	>50
3	P1	6.49	10.69	2.81	28.13
4	P2	1.58	1.65	1.22	17.35
5	nP1	1.75	1.53	1.08	8.46
6	nP2	0.53	0.99	0.32	7.71

In the formulations, nP1 and nP2 had the average hydrodynamic size of around 100 nm (figure 6). The expansion in the size of the nanoparticles obtained by DLS compared to FeSEM method can be accounted by the hydrophilic interaction of PVP molecules as similarly reported elsewhere [31]. The nP1 and nP2 formulations were stable with the zeta potential of −20.9 and −24.1 mV, respectively. The zeta potential values suggest that the nanoformulations were stable and suitable for biomedical applications.

3.3. Cytotoxicity

The cytotoxicity of P1, P2, nP1 and nP2 on different cell lines was evaluated and the results are shown in table 3 and figure 7.

The camphor thiosemicarbazone derivatives did not exhibit toxicity on all the tested cells. The RD cells were the most sensitive cells with the lowest IC_{50} for all samples. P1 and P2 exhibited toxicity on all the cell lines with the IC_{50} value range from 1.22 to 10.69 μg/ml. P2 was more toxic than P1. This fact can be related to the presence of phenyl group in the P2 molecule. Especially, the toxicity of nP1 and nP2 on the cancer cell increased compared to P1 and P2. The IC_{50} values of the nanoformulations were close to that of ellipticine for the cancer cell lines (Hep-G2, LU-1 and RD). For comparison, cisplatin (M = 300 g mol^{-1}) had the IC_{50}

value on Hep-G2 cell lines at 15.9 μM or 4.77 μg ml^{-1} [32]. Another research on camphor thiosemicarbazone complexes of Cu, Zn and Pd showed that their IC_{50} values on MCF-7 cells were 9.8, 12.9 and 14.0 μM, respectively [21]. Although the complexes and their nanoformulations exhibited toxicity on normal cells (Vero cell line), their toxicity was lower than that of positive control ellipticine. These results confirmed that our complexes and their nanoformulations are potential for cancer therapy.

4. Conclusion

In conclusion, the complex of camphor thiosemicarbazone derivatives with Pt(II) and their nanoformulations were successfully synthesised. The FTIR, MS, UV–vis, NMR spectra and thermal analysis revealed that Pt coordinated with two molecules of thiosemicarbazone derivatives through S and N atoms to form square planar structure. The new complexes and their nanoformulations inhibited all the investigated cancer cell lines with IC values ranging from 0.32 to 10.69 μg.ml^{-1}. These results showed that these materials, especially the nanoformulations, can be served as potential cancer drugs.

Declaration of interest

The authors report no declarations of interest.

References

[1] Ali I, Wani W A, Saleem K and Haque A 2013 *Anticancer Agents Med. Chem.* **13** 296
[2] Rajeswaran A, Trojan A, Burnand B and Gianneli M 2008 *Lung Cancer* **59** 1
[3] Pinzani V, Bressolle F, Haug I J, Galtier M, Blayac J P and Balmès P 1994 *Cancer Chemother. Pharmacol.* **35** 1
[4] Boulikas T and Vougiouka M 2003 *Oncology Reports* **10** 1663
[5] Utku S, Topal M, Dogen A and Serin M S 2010 *Turk. J. Chem.* **34** 427
[6] Elhag F A A, Edress F M and El Diwani H I 2013 Synthesis of 5-benzimidazolylbenzofuran derivatives of expected biological activity *1st Annual Int. Interdisciplinary Conf.* pp 867–72
[7] Komeda S, Lutz M, Spek A L, Chikuma M and Reedijk J 2000 *Inorg. Chem.* **39** 4230
[8] Aryal S, Hu C J and Zhang L 2010 *ACS Nano* **4** 251
[9] Avgoustakis K, Beletsi A, Panagi Z, Klepetsanis P, Karydas A G and Ithakissios D S 2002 *J. Control. Release* **79** 123
[10] Nejati-Koshki K, Mesgari M, Ebrahimi E, Abbasalizadeh F, Aval S F, Khandaghi A A, Abasi M and Akbarzadeh A 2014 *J. Microencapsul.* **31** 815

Adv. Nat. Sci.: Nanosci. Nanotechnol. **12** (2021) 025016

T H T Phan *et al*

[11] Cheng Y *et al* 2018 *Int. J. Pharm.* **545** 261
[12] Timothy C J, Kogularamanan S and Stephen J L 2016 *Chem. Rev.* **116** 3436
[13] Mizumura Y, Matsumura Y, Hamaguchi T, Nishiyama N, Kataoka K, Kawaguchi T, Hrushesky W, Moriyasu F and Kakizoe T 2001 *Jpn. J. Cancer Res.* **92** 328
[14] Mattheolabakis G, Taoufik E, Haralambous S, Roberts M and Avgoustakis K 2007 *Eur. J. Pharm. Biopharm.* **71** 190
[15] Phan T H T, Nguyen H D, Le T T, Nguyen L T and Ha T N T 2018 *Vietnam J. Sci. Tech.* **56** 75
[16] Ha P T *et al* 2013 *J. Nanomater.* **2013** 768628
[17] Kumar M and Ando Y 2007 *J. Phys. Conf. Ser.* **61** 643
[18] Gafer H E and Khalifa M E 2015 *Molecules* **20** 21982
[19] Saloutina L V, Zapevalov A Y, Kodess M I, Saloutin V I and Chupakhin O N 2001 *Russ. J. Org. Chem.* **37** 1522
[20] Giorgo P 2010 *Open Crys. J.* **3** 16
[21] Kokina T E, Sheludyakova L A, Eremina Y A, Vorontsova E V, Glinskaya L A, Piryazev D A, Lider E V, Tkachev A V and Larionov S V 2019 *Polyhedron* **163** 121
[22] Kumar M and Ando Y 2003 *Diam. Relat. Mater.* **12** 1845
[23] Rezvantalab S, Drude N I, Moraveji M K, Güvener N, Koons E K, Shi Y, Lammers T and Kiessling F 2018 *Front. Pharmacol.* **9** 1260

[24] Skehan P, Storeng R, Scudiero D, Monks A, McMahon J, Vistica D, Warren J T, Bokesch H, Kenney S and Boyd M R 1990 *J. Natl. Cancer Inst.* **82** 1107
[25] Likhitwitayawuid K, Angerhofer C K, Cordell G A, Pezzuto J M and Ruangrungsi N 1993 *J. Nat. Prod.* **56** 30
[26] Kokina T E, Sheludyakova L A, Eremina Y A, Vorontsova E V, Glinskaya L A, Piryazev D A, Lider E V, Tkachev A V and Larionov S V 2017 *Russ. J. Gen. Chem.* **87** 2332
[27] Zouchoune B and Mansouri L 2019 *Struct. Chem.* **30** 691
[28] Al-Jibori S A, Barbooti M M, Al-Jibori M H S and Aziz B K 2017 *J. Mater. Environ. Sci.* **8** 1365
[29] Guo H, Lai Q, Wang W, Wu Y, Zhang C, Liu Y and Yuan Z 2013 *Inter. J. Pharm.* **451** 1
[30] Torchilin Vladimir P 2009 Passive and Active Drug Targeting: Drug Delivery to Tumors as an Example *Drug Delivery* (New York, NY: Springer) 3–53
[31] Leuschner C and Kumar C 2005 *Nanoparticles for Cancer Drug Delivery.* **2005** 289–326
[32] Pascale F, Bedouet L, Baylatry M, Namur J and Laurent A 2015 *Anticancer Res.* **35** 6497